

Study the Parametric Effect on Austempered Ductile Iron

¹Dr.Gaurav Saini, ^{2*}Dr.Abhishek Chauhan, ³Sandeep Goyal

^{1,2}*Department of Mechanical Engineering, UIET, Panjab University SSG Regional Centre, Hoshiarpur, Punjab 146021, India.*

³*Punjab Engineering College (Deemed to be University), Sector 12, Chandigarh, 160012, India.*

**Corresponding author : mecherabhishek @yahoo.co.in*

Abstract

A study was conducted to analyze the effects of the traditional austempering process on microstructural characteristics, including hardness and abrasion wear resistance, of austempered ductile iron (ADI). Two batches of cubical samples measuring (10x10) were prepared from an alloyed nodular ductile cast iron and were initially subjected to austenitization at 900°C for a duration of 120 minutes. In a salt bath, both sample batches were austempered at four distinct temperatures: 240°C, 270°C, 300°C, and 330°C. But the austempering time of both the batches were kept different, for first batch it was 90 minutes and for second batch austempering time was 120 minutes. The test results shows that with increase in austempering temperature wear resistance of ADI decreases and same variation is observed with the increase in austempering time. The findings indicate that the hardness of ADI diminishes as the austempering time and temperature increase. According to the ADI's microstructural examination, the size of the bainite and martensite found in the ADI increases as the austempering temperature rises, indicating that the structure gets coarser.

Keywords: Austempered Ductile Iron (ADI), Austempering temperature, Austempering time, Wear resistance, Hardness.

Introduction

Austempered ductile cast iron (ADI) has become an essential engineering material in recent years due to its appealing qualities. These include great wear resistance, high fatigue strength, fracture toughness, and good ductility at high strength. These benefits have led to the widespread usage of ADI in numerous structural and wear-resistant applications in the automotive, defense, and

earthmoving machinery industries, among others. Due to its better stress/cost ratio, it also enables the conversion of many steel assemblies to ductile iron. [1-10]. X.Guo et.al [11] shown that the alloying elements and cooling rate both affect the amount of pearlite. According to recent research [12], ADI may find usage in situations where impact loads and wear are present. Austenitization involves holding the ductile iron in muffle furnace maintained at a suitable temperature in austenite range (generally 850 - 950°) to obtain complete transformation of the matrix of ductile iron to austenite and its homogenization in respect of carbon and alloying element. The effect of increased pearlite content On reducing the austenization time is apparent [13] the diffusion time require for austenization depends on temperature , nodule count ,matrix structure, diffusivity of carbon, alloy content and its segregation in iron.

Experimental Details

Alloyed nodular cast iron with a typical composition was used for the studies. The ductile iron composition given in Table 1 was tested by spectrometer. Samples are made from the Y blocks casted for the purpose as shown in Figure1.

Table 1: Composition of ductile iron

Element	C	Mn	Si	S	P	AL	Cu	Cr
Wt%	3.341	0.285	3.345	0.015	0.026	0.021	0.804	0.012
Element	Mo	Ni	Pb	Ti	V	W	Fe	Mg
Wt%	0.000	0.253	0.01	0.011	0.000	0.041	91.859	0.030

Specimens of size 10mmx10mmx15mm were machined from given block with dimensions as prescribed by ASMT.



Figure 1. The shape and dimensions of specimens used

Experimental Setup

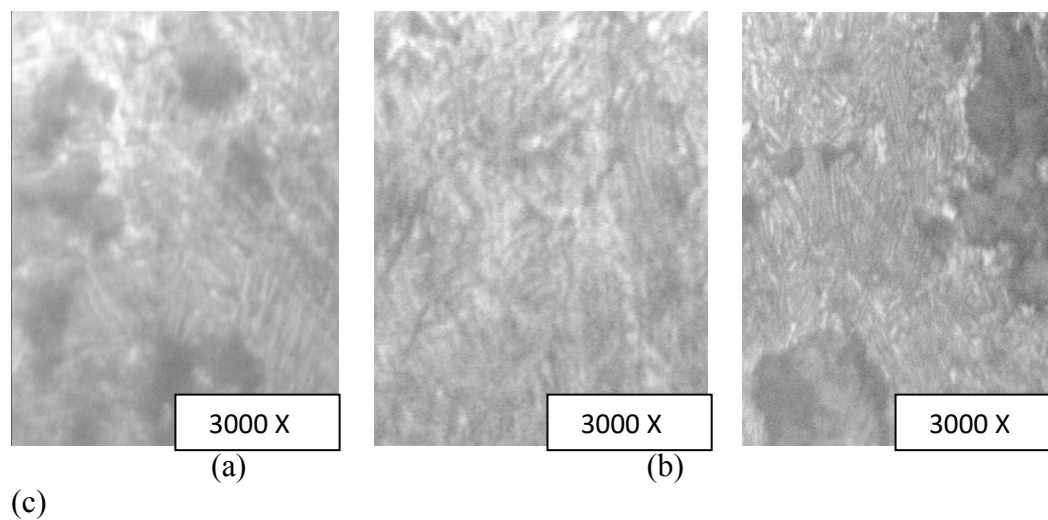
- Programmable heat treatment furnace.
- Salt Bath Furnace (KNO₃ & NaNO₃).

(50% + 50%)

- c. Optical image analyzer.
- d. Vickers hardness \tester.
- e. Wear Testing Machine.
- f. Spectroscope (D.R. Spectrometer)
- g. X- Ray diffractometer (XPERT-PRO).

4. Microstructural Analysis

Figure 2 shows microstructure of heat treated sample through the magnification of 3000 X under a microscope and table 2 distinguishes all the samples according heat treatment parameters. Microstructure analysis reveals that bainite has formed in every sample. The structures also demonstrate the carburization of the samples, with the exception of sample number five, which exhibits a white area that indicates decarburization. This can be reasoned to that the sample was outside carburizing bed during austenitization process. The size of the bainite and martensite found in the ADI samples increased as the austempering temperature rose, according to an analysis of all the samples. This lead to the coarsening of structure. This coarsening on size was confirmed by performing X-ray diffraction analysis on all the samples and by calculating the size of bainite. For samples 1, 2, and 3, the bainite needle size stays around the same (.0210), but for samples 4 and 5, it slightly increases, and as we proceed to sample no. 8, which has the highest austempering temperature and time, the size increases significantly to.0316. As shown in table 3. In this sample 5 decarburized as it was outside carburized bed.



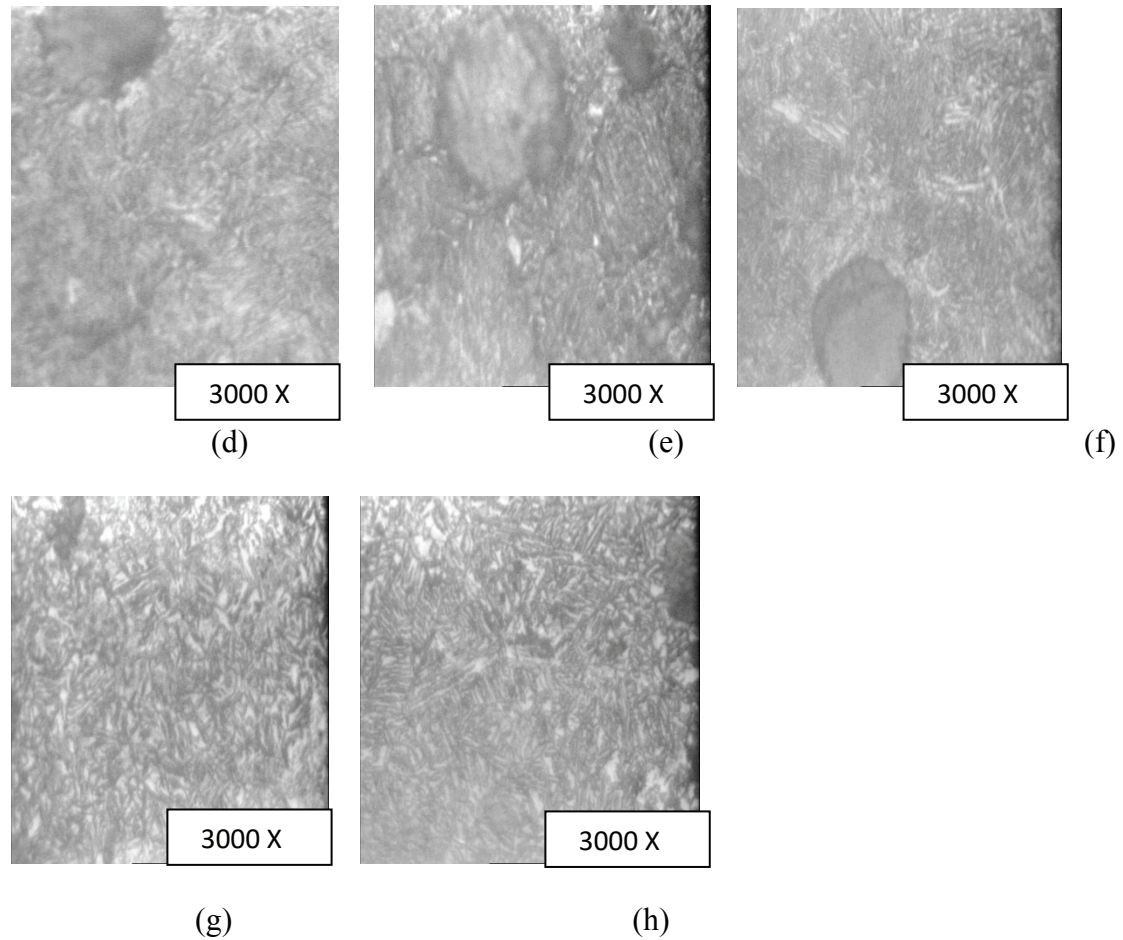


Figure 2. Samples' microstructure under an optical microscope demonstrating the production of bainite. (a) sample 1 finer structure, (b) sample 2 finer structure, (c) sample 3 finer structure and shows carburization, (d) sample 4 medium size needle, (e) sample 5 shows decarburized sample, (f) sample 6 medium needle and carburization (g) sample 7 coarser structure, (h) sample 8 coarser structure.

Table 2. The austempering time and temperature of each sample

Sample no.	Austempering Temp. (°C)	Austempering Time. (min.)
1	240	90
2	240	120
3	270	90
4	270	120
5	300	90
6	300	120
7	330	90
8	330	120

Figure 2 shows microstructure of heat treated sample through the magnification of 3000 X under a microscope and table 2 distinguishes all the samples according heat treatment parameters. Microstructure analysis reveals that bainite has formed in every sample. The structures also demonstrate the carburization of the samples, with the exception of sample number five, which exhibits a white area that indicates decarburization. This can be reasoned to that the sample was outside carburizing bed during austenitization process. By examining every sample, it was discovered that when the austempering temperature rises, the size of the bainite and martensite found in the ADI samples increases. This lead to the coarsening of structure. This coarsening on size was confirmed by performing X-ray diffraction analysis on all the samples and by calculating the size of bainite. For samples 1, 2, and 3, the bainite needle size stays around the same (.0210), but for samples 4 and 5, it slightly increases, and as we proceed to sample no. 8, which has the highest austempering temperature and time, the size increases significantly to.0316. As shown in table 3. In this sample 5 decarburized as it was outside carburized bed.

5.Hardness Testing

Figure 3 illustrates how the ADI's austempering temperature affects the samples' hardness. The graph clearly shows that when the austempering temperature rises, hardness falls. In the graph upper line shows the variation in hardness for samples at 240,270, 300 and 330°C for 90 minutes and lower line for 120 minutes of same temperature range. As we can see graph is very similar for both time range. But samples austempered for 90 minutes shows more hardness for similar austempering temperature throughout the temperature range. These findings support the notion that when the austempering temperature rises, both austenite and ferrite get coarser. The hardness significantly decreased as a result of the coarse grains created at higher temperatures. There is coarsening of structure with increase in austempering temperature, with this hardness decreases as there more of graphite comes on the surface . As also seen in microstructure of sample 5 there is drastic decarburization which also helps in decrease of hardness to a certain extent.

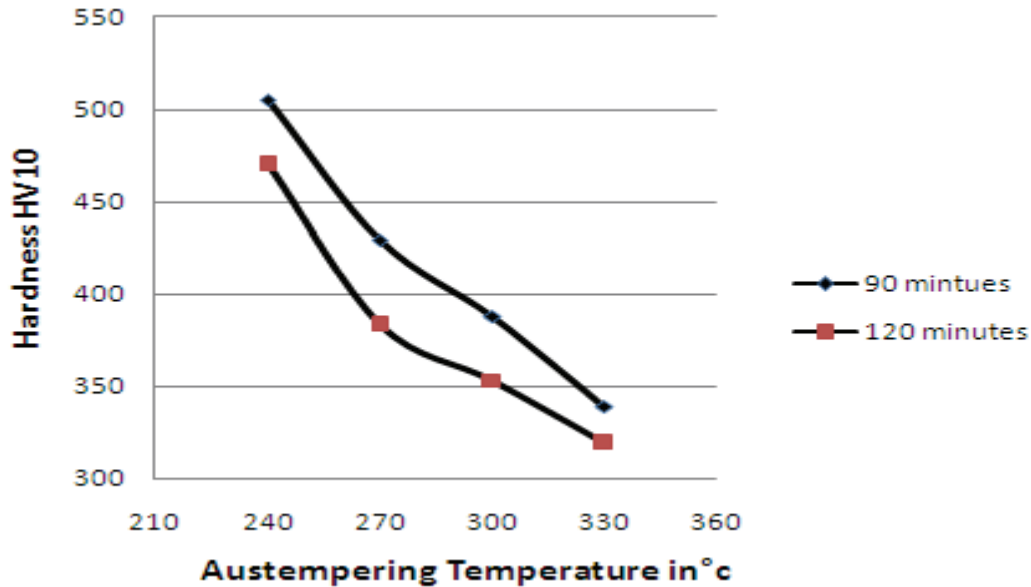


Figure 3. The hardness variation w.r.t. austempering temperature

5.1.Abrasive Wear Resistance Test

The wear loss in the ADI samples at predetermined temperatures and times is displayed in Figure 4 (a),(b),(C) and (d). As the wear test was performed for 4 hours the graph a,b,c and d in figure 4 show readings after 1,2,3 and 4 hour of wear test respectively for all the samples. Wear loss is comparable during the first hour of heat treatment for both 90 and 120 minutes, and it increases as the austempering temperature rises from 240 to 270° C. It then slightly decreases as the austempering temperature rises to 300° C, and it accelerates when the temperature reaches 330° C. As we can see by studying all the graphs wear loss is more prominent in first hour of wear testing. The trend of wear loss after elapse of one hour shows wear loss is less at low austempering temperature and it increases with rise in the same. Wear loss is lower for 90-minute samples at 240 and 270° C than for samples taken at 120° C for 1 to 2 hours of wear, but it stays the same as the temperature rises further for both time periods. Wear loss is maintained for 90 and 120 minutes at 240 and 270° C during the third hour of wear. After that, when the temperature is raised to 300° C, the 90-minute sample experiences extremely significant wear loss, but only slightly for the 120-minute sample, and when the temperature rises to 330° C, there is only a slight increase in wear for both timings. These readings are also very consistent with hardness variation as we can see that hardness decreases with increase in temperature. In the last hour with wear loss maintained between 120 to 180 micron the readings of 240 and 270° C became constant for both 90 and 120 minutes. Infact wear was constant with further increase in temperature of 120 minutes sample but it increases consistently for 300° C of 90 minutes sample but shows marginal increase in wear loss for 330° C and 90 minutes sample. When examining each sample separately, we can observe that wear loss rises as testing duration

increases, but it starts out quickly before increasing steadily over time. The reason for the anomaly in sample 5 (300°C, 90-minute austenitizing temperature) is that the structure experienced a significant decarburization during the austenitizing process. It is quite likely that the sample must have remained outside the carburizing bed during austenitization, which led to carbon loss and a reduction in the sample's wear resistance.

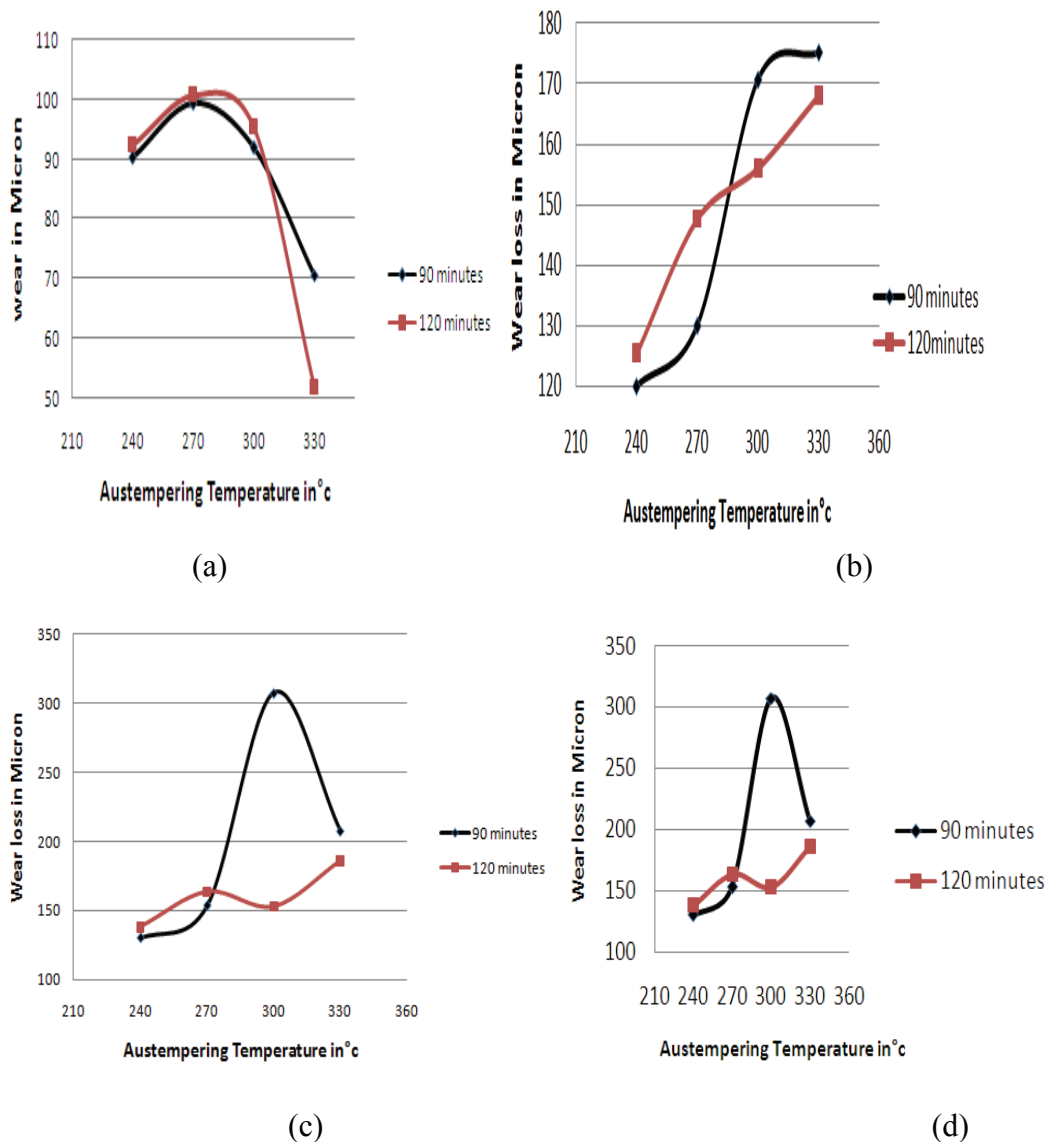


Figure 4. Wear loss varies with the change in austempering temperature and time. After (a) one hour (b) Two hours (c) Three hours (d) Four hours

6. X-Ray Diffraction

Table 3. Particle size calculation of austenite

Sample no.	2 θ	Θ	Cos θ	$d\alpha=0.9\lambda/B$ Cos θ
1	44.9647	22.4823	0.92399	.0290
2	44.8450	22.4225	0.92439	.0290
3	44.9680	22.4840	0.92398	0.290
4	44.9741	22.4870	0.92396	0.308
5	44.7055	22.3527	0.92485	0.308
6	44.9756	22.4878	0.92396	0.327
7	44.8339	22.4129	0.92443	0.327
8	44.8258	22.4129	0.92446	0.327

X-ray diffraction analysis performed on the samples gives to peaks for all the samples as shown in figure 5. The position of the peak is shown on the horizontal line(2 θ). The first peak in all the sample comes around 44° which leads to to fact that martensite is present in all the sample and second peak is at 82° approximately for all the samples showing formation of bainite. This analysis was used to calculate the size of bainite and martensite as calculated in table 3 and 4 respectively. This calculation shows coarsening of structure as austempering temperature increases. It can be seen that size of bainite and martensite for samples 1, 2 and 3 remains same but as the is increased further size of particles increases a little but there is a notable change in the size for sample 6, 7 and 8 as it increases to .0316 for bainite and .0327 for martensite. The detailed data of measurement conditions, position for each sample and area covered is attached in the appendix. Individual graph of each sample with every peak shown is also attached to the appendix. Austenitization time also affected the coarsening of samples as seen in the case of sample 3 and 4 and samples 5 and 6 there was increase in the size of bainite and martensite with increase in austenitization time.

Table 4. Particle size of ferrite

Sample No	2 θ	Θ	Cos θ	$d\gamma=0.9\lambda/B$ Cos θ
1	82.4987	41.2493	0.7518	0.0210
2	82.4968	41.2484	0.7518	0.0210
3	82.7666	41.3833	0.7503	0.0210
4	82.4600	41.2300	0.7520	0.0225
5	82.6153	41.3076	0.7511	0.0243
6	89.5199	44.7599	0.7100	0.0334
7	82.4370	41.2185	0.7522	0.03160
8	82.6239	41.3119	0.7511	0.03160

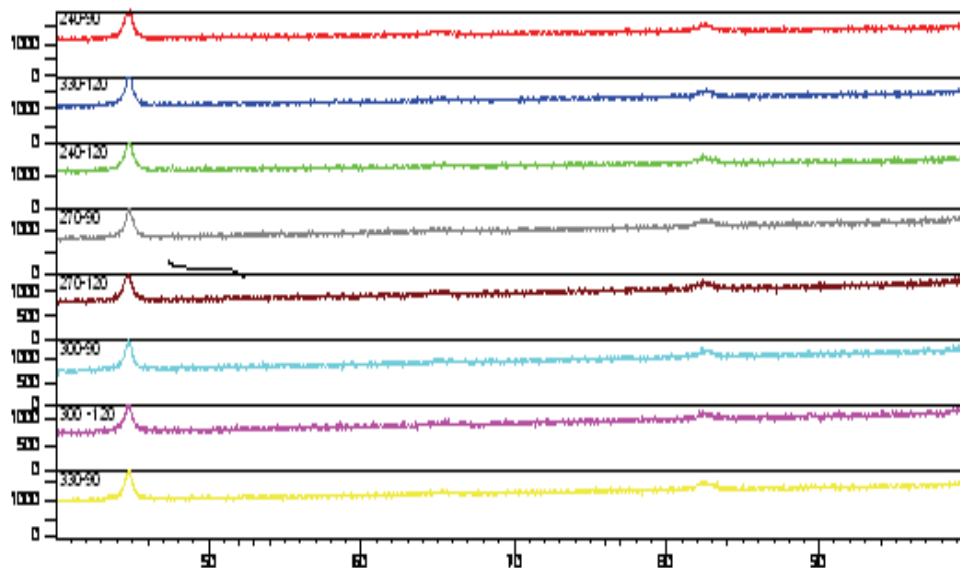


Figure 5. Peaks of Bainite and martensite given by XRD analysis.

7. Wear Track

While studying the wear track it was seen in Figure 6 that in general wear path got wider with increase in the austempering temperature. As in sample 1 the path lines are very fine as compared to other samples, as we reach to sample 5 which show more wear can be due to the reason of decarburization of sample. Sample 7 and 8 shows maximum wear as the austempering temperature was maximum for these two samples. The wear track variation can be contributed to the coarsening of samples with increase in austempering temperature. As for sample 1, 2, and 3 the particle size is small and also samples are harder the wear becomes difficult and coefficient is less so particle removed from the surface are finer and wear track is also finer. And for sample 4 to 8 particle size increases and from hardness data we can also see that hardness also decreases with increase in austempering temperature so *cof* increases which can be reasoned for wider wear track shown by these samples. In this it can also be seen that as the track becomes wider and coarser the amount of wear also increases proportionally. When comparing sample 1 and 2 we can see that wear is more and track is getting wider similar changes can be seen between sample 3 and 4 and sample 7 and 8, this shows that austempering time has significant effect on the wear track which corresponds to the fact that austempering time also effect the coefficient of friction as the austempering time is increased from 90 min. to 120 min. coefficient of friction increases and wear track becomes wider. The exception in the comparison of sample 5 and 6 is because of the fact that sample 5 is decarburized during austenitization process because it is assumed that it remained outside carburizing belt.

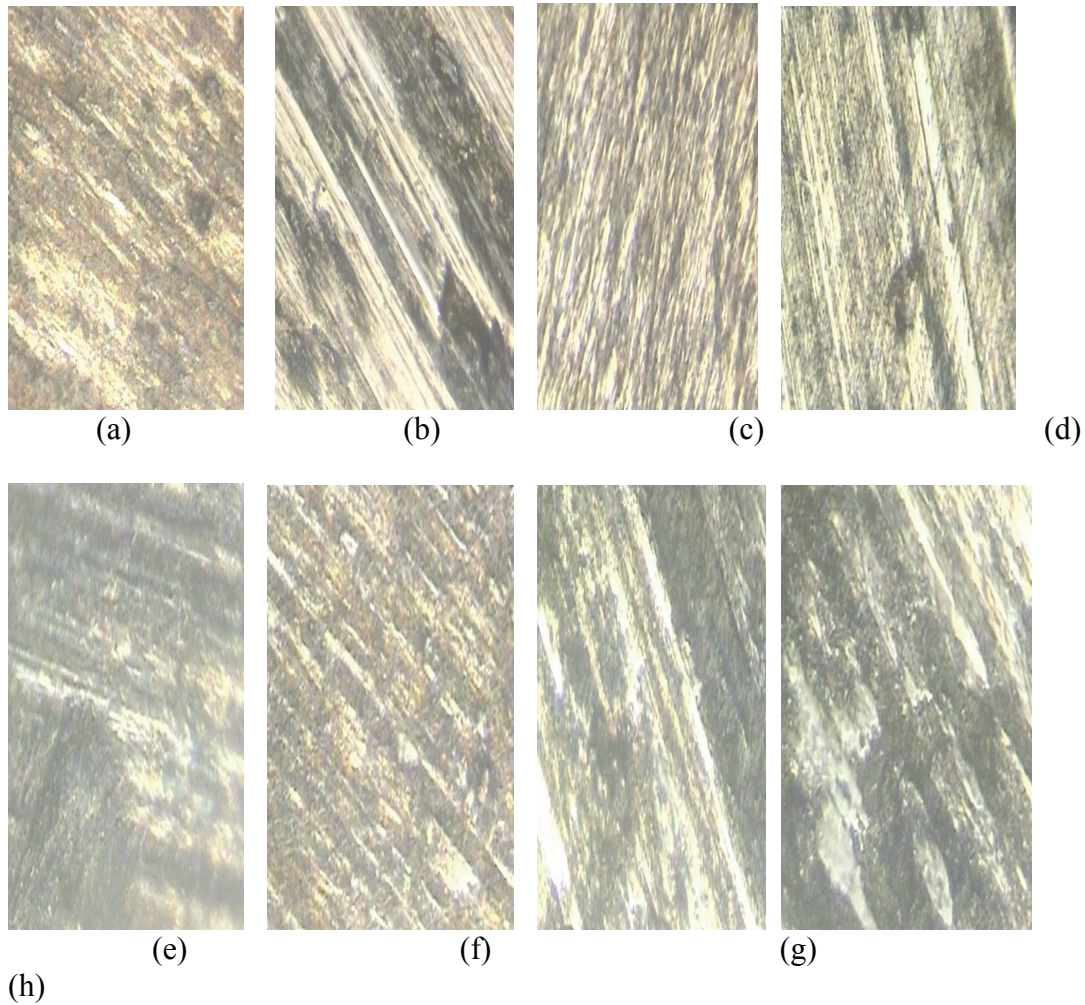


Figure 6. Wear track under optical microscope for sample (a) 1, (b) 2, (c) 3, (d) 4, (e) 5, (f) 6, (g) 7, (h) 8

8. Conclusions

Austempering temperature and time effects were investigated. Evaluations were made of the microstructure, hardness, and resistance to abrasive wear. The study has led to the following conclusions.

- XRD studies show that the microstructure of austempered ductile iron (ADI) becomes coarser with increase in the time and temperature of austempering.
- The hardness of austempered ductile iron (ADI) diminishes with increase in the time and temperature of austempering
- With increase in the time and temperature of austempering abrasion resistance of austempered ductile iron (ADI) falls. However, sample no. 5 sudden abrasion resistance behavior is

explained by the decarburization that had place throughout the austenitization procedure.

References

- [1] Górný, Marcin, et al. "Structural stability of thin-walled austempered ductile iron castings." *Archives of Civil and Mechanical Engineering* 23.2 (2023), pp 79.
- [2] Krawiec, Halina, et al. "Influence of heat treatment parameters of austempered ductile iron on the microstructure, corrosion and tribological properties." *Materials* 16.11 (2023), pp 4107.
- [3] Sabzalipour, Mohsen, and A. M. Rashidi. "Machinability of martensitic and austempered ductile irons with dual matrix structure." *Journal of Materials Research and Technology* 26 (2023), pp 6928-6941.
- [4] Wang, Bingxu, et al. "Microstructure, wear behavior and surface hardening of austempered ductile iron." *Journal of Materials Research and Technology* 9.5 (2020), pp 9838-9855.
- [5] Upadhyaya, Rajat, Kamlesh Kumar Singh, and Rajeev Kumar. "Study on the effect of austempering temperature on the structure-properties of thin wall austempered ductile iron." *Materials Today: Proceedings* 5.5 (2018), pp 13472-13477.
- [6] Olawale, J. O., and K. M. Oluwasegun. "Austempered ductile iron (ADI): a review." *Materials performance and characterization* 5.1 (2016), pp 289-311.
- [7] Kumari, U. Ritha, and P. Prasad Rao. "Study of wear behaviour of austempered ductile iron." *Journal of Materials Science* 44 (2009), pp 1082-1093.
- [8] Erić, Olivera, et al. "The austempering study of alloyed ductile iron." *Materials & design* 27.7 (2006), pp 617-622.
- [9] El-Din, H. Nasr, et al. "Ausforming of austempered ductile iron alloyed with nickel." *International Journal of Cast Metals Research* 19.3 (2006), pp 137-150.
- [10] Haseeb, A. S. M. A., Md Aminul Islam, and Md Mohar Ali Bepari. "Tribological behaviour of quenched and tempered, and austempered ductile iron at the same hardness level." *Wear* 244.1-2 (2000), pp 15-19.
- [11] Guo, X., et al. "A mechanical properties model for ductile iron." *TRANSACTIONS-AMERICAN FOUNDRYMENS SOCIETY* (1998), pp 47-54.
- [12] Soedarsono, Johnny Wahyuadi, et al. "Effect of the austempering process on thin wall ductile iron." *Journal of Materials Science and Engineering A: Structural Materials: Properties, Microstructure and Processing* 1.2 (2011), pp 236-242.
- [13] García, Javier Hidalgo, and Kenneth Hamberg. "Improving the Fracture Toughness of Dual-phase Austempered Ductile Iron." *Chalmers University of Technology. Department of Materials and Manufacturing Technology* 82 (2008), pp 23-26.